



Seventh Framework Programme FP7-SPACE-2010-1  
 EU-Russia Cooperation in GMES (SICA)

Grant agreement for: Collaborative Project

Project acronym: **MAIRES**

Project title: **Monitoring Arctic Land and Sea Ice using Russian and European Satellites**

Grant agreement no. 263165

Start date of project: 01.06.11

Duration: 36 months

Project coordinator: Nansen Environmental and Remote Sensing Centre, Bergen, Norway

**D5.1: Iceberg maps from satellite data**

Due date of deliverable: 31.05.2013

Actual submission date: 01.07.2013

Organization name of lead contractor for this deliverable: NERSC

Project co-funded by the European Commission within the Seventh Framework Programme, Theme 6 SPACE		
Dissemination Level		
PU	Public	X
PP	Restricted to other programme participants (including the Commission)	
RE	Restricted to a group specified by the consortium (including the Commission)	
CO	Confidential, only for members of the consortium (including the Commission)	

ISSUE	DATE	CHANGE RECORDS	AUTHOR
0	01/07/2013	Version 0.1	S. Sandven, V. Alexandrov, M. Babiker,

### **MAIRES CONSORTIUM**

Participant no.	Participant organisation name	Short name	Country
1 (Coordinator)	Nansen Environmental and Remote Sensing Centre	NERSC	NO
2	JOANNEUM RESEARCH Forschungsgesellschaft mbH	JR	AU
3	Scientific foundation Nansen International Environmental and Remote Sensing Centre (NIERSC)	NIERSC	RU
4	Moscow State University of Geodesy and Cartography	MIIGAIK	RU

No part of this work may be reproduced or used in any form or by any means (graphic, electronic, or mechanical including photocopying, recording, taping, or information storage and retrieval systems) without the written permission of the copyright owner(s) in accordance with the terms of the MAIRES Consortium Agreement (EC Grant Agreement 263165).

All rights reserved.

This document may change without notice

## Table of Contents

1	INTRODUCTION.....	3
2	REMOTE SENSING DATA FOR ICEBERG DETECTION.....	4
3	METHODOLOGICAL FOUNDATION OF ICEBERG DETECTION FROM SATELLITE IMAGES:.....	6
3.1	ICEBERGS IN SEA SURFACE .....	6
3.2	ICEBERGS AMONG FAST ICE.....	7
3.3	ICEBERGS IN DRIFTING ICE.....	9
4	COMPARISON OF DATA ON ICEBERG DISTRIBUTION, DERIVED FROM SATELLITE IMAGES WITH HISTORICAL DATA .....	13
5	CONCLUSIONS.....	14

### List of Figures

Figure 1	ENVISAT ASAR Wide Swath subimage (HH-polarization) of the northeastern Barents Sea for September 15, 2006 (a) and map of iceberg distribution to the south of FJL, composed from ENVISAT ASAR image for September 15, 2006 (b). .....	7
Figure 2	ENVISAT SAR images of Hornsund area in Svalbard and photo of iceberg, April 2004. a) ASAR WS image for 01.04.2004; b) photo of observed iceberg, detected in SAR images; images in APP mode for 15.04.2004: c) – at VV-polarization and d) at HH-polarization. Bright points, corresponding to icebergs, are delineated. ....	8
Figure 3	Images of icebergs in fast ice of FJL. a) ENVISAT ASAR subimage for April 5, 2006, b) Landsat subimage for April 14, 2006, c) “Monitor-E” subimage for April 7, 2006. ....	9
Figure 4	ENVISAT IMM subimage, covering an area west of Vilkitsky Strait (a) and iceberg distribution map, composed from analysis of this image, October 14, 2006 (b). Crosses correspond to locations of icebergs, observed in this area in late September.....	10
Figure 5	Images of icebergs in Inostrantseva Bay: ENVISAT ASAR WS for March 31 (a), April 01 (b), April 18 (c), April 22 (d), April 25 (e), May 11 (f) and Landsat visible image for April 23, 2006 (g).....	11
Figure 6	Three visible Aster images for April 20, 2005, overlaid on the map of northeastern Barents Sea. Detected icebergs are marked by dots.....	13

### List of Tables

Table 1: XXXX.....	Error! Bookmark not defined.
--------------------	------------------------------

## SUMMARY

This report deals with studies of iceberg identification among open water, fast ice and drifting ice using visible Landsat, "Monitor-E", ASTER and MODIS images and synthetic aperture radar (SAR) images. The possibility of identification of Arctic icebergs in satellite images of different types is estimated, and features for iceberg detection in these images are determined. Several examples of satellite image analysis are presented. The technological schemes of combined use of different types of satellite information depending on ice and hydrometeorological conditions are proposed. The perspectives of development of iceberg detection methodology are outlined.

## 1 Introduction

The importance of iceberg studies in the Arctic is determined not only by pure scientific interest, but also exploration of the Arctic shelf, because icebergs are dangerous for navigation, oil and gas platforms and underwater communications. Icebergs, formed in the Russian Arctic, are calved from outlet glaciers, located in Svalbard, Franz Josef Land (FJL), Novaya Zemlya and Severnaya Zemlya, and exported to the Arctic Basin, or to the south – to the Barents, Kara and Laptev Seas, where they melt during several years [1]. FJL has the largest iceberg. Large icebergs are calved from glaciers, located in George Land and Wilczek Land and usually are located in shallow areas near the fronts of outlet glaciers [2]. Icebergs with length of several hundred meters and 60-100 m high were observed in FJL Straits: British Channel, Cambridge, Yermak, Austrian Channel, Zubova and several others. Svalbard, particularly, Negribreen, Stonebreen, and Brasvelbreen in North-Eastern Land are also one of the main iceberg sources in the Barents Sea [3]. Icebergs, formed in Novaya Zemlya archipelago, mainly melt in fjords and are rarely observed in the open sea [4].

Icebergs in the Eurasian Arctic seas are significantly smaller than those in the Antarctic and Greenland. Their average length and width in the Barents Sea amounts to 64 m and 46 m according to ship observations, and 103 m and 16 m, according to air reconnaissance data, Their maximum sizes amounts to 180 m and 30 m, and 700 m and 50 m, respectively [5].

The amount of observed icebergs is characterized with significant interannual and seasonal variability. During the period of their most regular observations (1936 - 1993) their maximum number was observed in 1955, 1960, 1987, and 1991 [5]. Near Brasvelbreen glacier particularly large number of icebergs (more than 100) was observed in 1937 [6], as well as in 1987 and 1988. In 1988 about 200 icebergs were observed in the eastern part of Spitsbergen bank, 50-60 of them were grounded [3, 7]. During Russian-Norwegian expedition onboard R/V "Akademik Shuleykin" in August 1989 62 icebergs were observed, and 28 of them in the western Barents Sea, mainly around Hopen and Kong Karl Land [8]. In late August this year, 17 icebergs were observed in Kong Larl Land region. During Norwegian R/V "Lance" cruise in July-August 1990 about 350 icebergs were observed, their largest number (192) – between 38° E and 48° E [9]. In July-August of the same year during R/V "Professor Multanovsky" cruise 45 icebergs and growlers were observed in the Barents Sea, their maximum number was observed near the ice edge to the north of 78,5° N [10]. During the «Lance» cruise in August 1991 59 icebergs were observed, ten of them longer than 100 m [11]. In August 1993 totally 23 icebergs with size from 30 m to 200 m were observed in FJL region, and in May 2003 – their large amount was found in the area near Shtokman gas deposit [12, 13]. Their average size amounted 72 x 120 m, and maximum size – 190 x 430 m.

It is evident from afore-mentioned examples that iceberg distribution in the Arctic seas is irregular, and areas, where they were met more often, are close to outlet glaciers. At the same time, icebergs can be met far from them. The 50 m isobath is located relatively near from the shores of the main arctic archipelagos, and only in some parts (eastern part of FJL, for example), depths near shores can be significantly more. Therefore, icebergs and growlers less than 50-m draft drift over the whole Barents and Kara Seas [14] in accordance with a general scheme of water and ice circulation. Their trajectories, influenced by ocean currents, tides, wind and bottom relief, are complex and represent a sum of translation and rotation.

## 2 REMOTE SENSING DATA FOR ICEBERG DETECTION

Icebergs are well detected from high-resolution visible images from Landsat, Aster, “Monitor-E” and other satellites, received in light conditions in absence of clouds. From multispectral Landsat TM (Thematic Mapper) images, covering an area of 183 x 182.8 km with 30 m resolution, the fourth channel with a wavelength of 0.8 mc is the most informative [2]. The iceberg identification is difficult when their size is about the sensor resolution, and when their size corresponds to 2-3 pixels (60-90 m), they are identified using one of the following features:

- presence of shadow,
- light patch – light reflection from sunny part of iceberg,
- texture of large tabular icebergs,
- presence of fracture near the iceberg due to its motion relatively ice.

Weather conditions, first, cloudiness and sun height, which determine a length of iceberg shadow and contrast between sunny side of iceberg and its surroundings, influence manifestation of these features. Icebergs are better detected in early spring, when they are surrounded with level ice and have long shadow due to small Sun angles [2]. The valuable complementary information for their detection provide tracks in sea ice in the form of ellipse [7], caused by tidal currents or inertial movements.

Let us suppose that in visible images from other satellites it is also possible to detect icebergs with size 2-3 times more than spatial resolution. Therefore from panchromatic images from Russian “Monitor-E” satellite with 8-10 m resolution icebergs of 20-25 m size can be recognized, from multispectral images with 20 m resolution –more than 40-50m. Icebergs with size more than 30-35 m will be identified from ASTER images with 15 m resolution, and from Terra and Aqua MODIS images with 250 m resolution - longer than 500 m. Icebergs of that size are rarely observed in the Arctic, but they are the most dangerous for drilling platforms and underwater communications.

The possibility of iceberg detection from radar images depends on difference of their backscatter with that of surrounding water surface or sea ice, which depends also on wavelength, polarization and incidence angle. In radar images, they are shown as points or small patches with brightness significantly more than multiyear ice brightness [15-17]. The following factors influence a possibility of their detection in synthetic aperture radar (SAR) images: 1) size, form, and orientation of iceberg; 2) characteristics of its surface – presence of ridges, cavities, cracks; 3) internal heterogeneities (inclusions of air bubbles and fragments of rocks); 4) presence of fresh water on its surface; 5) presence of real or seeming shadow; 6) state of surrounding sea surface or ice cover; 7) presence of open water area behind iceberg when it is streamlined by ice; 8) presence of track in drifting ice, and 9) presence of wave track. With wind speed less than  $5 \text{ ms}^{-1}$  or more than  $11 \text{ ms}^{-1}$  and absence of the sea ice from ERS-1 SAR images practically all icebergs longer than 120 m can be detected, three fourth of average (60-120 m) and approximately half of small icebergs (15-60 m) [18]. ERS-1 SAR parameters are not optimal for solving this task, and for this purpose using SAR, operating at HH-polarization with larger incidence angles, specifically RADARSAT-1 SAR, is preferable. Images in Wide mode (25 m resolution) and ScanSAR Narrow B (50 m resolution), acquired in May-June in Newfoundland area, were analyzed in [19], and iceberg radar signatures were described based in comparison with subsatellite data. It was shown that icebergs with size approximately equal to SAR resolution are detected with incidence angles more than  $35^\circ$ , and larger icebergs even in wind-roughened sea surface. Iceberg detection in drifting ice is more complex, because they can have signature similar to that of some ice features. Several estimates of iceberg size, identified in SAR images, were done based on subsatellite observations. 500-m long and 50-100 m wide iceberg is

reliably detected in ERS-1 SAR image due to its bright tone and open water area in its western side [20]. According to work [21], icebergs with a length, less than 200 m are often cannot be detected in ERS-1 images due to speckle-noise. In Almaz-1 SAR images (wavelength 10 cm, HH-polarization, 10-15 m resolution and swath width of 40 km) icebergs longer than 40 m were detected reliably among fast ice and compact drifting ice [22]. According to work [23], detection of 1-km size icebergs in RADARSAT images present certain difficulties, bit it significantly simplified when a number of icebergs is observed in relatively small region. Shadow and characteristic track after icebergs in drifting ice, when their drift differs from that of surrounding ice, can be indirect features for their detection [15, 22-25].

A possibility to obtain multifrequency (X-, C- or L-bands) and multipolarization (VV, HH, VH, HV) allows obtaining more information about different sea ice and iceberg parameters. ALOS PALSAR is an L-band active microwave sensor. Its ScanSAR mode with swath width of 250-350 km (VV and HH-polarizations) is of greatest interest, and can be effectively used for solving this task. TerraSAR-X ScanSAR images (16-m resolution, 100 km swath width, different polarizations) also can be effectively used.

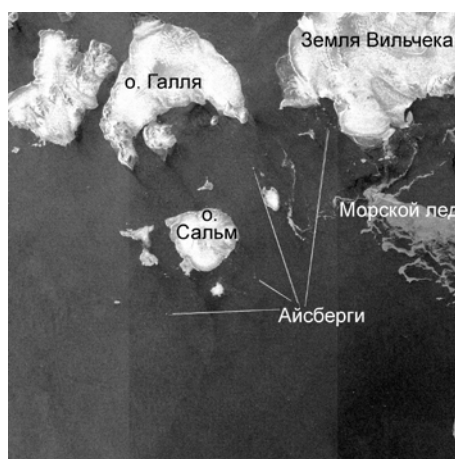
### 3 Methodological Foundation of Iceberg Detection From Satellite Images:

To estimate a possibility of identification of icebergs of different size from SAR data we have analyzed image series for icebergs located in open water, fast ice and drifting ice. Comparison of obtained data with subsatellite observations or near-simultaneous high-resolution visible images is necessary for estimates of reliability of obtained results.

#### 3.1 Icebergs in sea surface

As an example, we examine an ENVISAT ASAR Wide Swath image, covering the northeastern part of the Barents Sea between Franz Josef Land and Novaya Zemlya, acquired on September 15, 2006. Its subimage is shown in Figure 1. Drifting ice is seen to the south of FJL to the east of Wilczek Land meridian. Remaining part between FJL and Novaya Zemlya is covered with calm water surface. A large number of icebergs to the south of FJL and near Novaya Zemlya coast was detected among calm water surface, shown with dark tone in SAR image (Figure 1, a). In addition, their large number was found between islands of FJL archipelago. In the far-range, where the signal from calm water surface significantly increases, their identification is complicated.

This example shows a principal possibility of using 150-m resolution SAR for iceberg detection among calm water surface. An open question is correspondence of iceberg distribution map, composed by means of visual interpretation (Fig. 1b) and real conditions. Another open question is – icebergs of what size are detected in water surface, and what – not detected? Several ways can be used for their solving: 1) analysis of sequential SAR images for near days and comparison of composed maps, 2) joint analysis of near-simultaneous visible and SAR images, and 3) conducting subsatellite observations from ship or ice reconnaissance airplane (helicopter). Based on conducted analysis and average characteristics of their linear size in this region, it is possible as a first approximation to conclude, that size of icebergs, identified from image for September 15, 2006, is more than 70-80 m. Conducting detailed subsatellite experiments is necessary to define it more accurately.



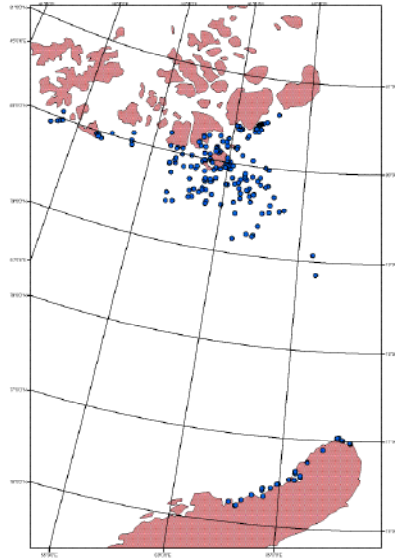


**Figure 1** ENVISAT ASAR Wide Swath subimage (HH-polarization) of the northeastern Barents Sea for September 15, 2006 (a) and map of iceberg distribution to the south of FJL, composed from ENVISAT ASAR image for September 15, 2006 (b).

### 3.2 Icebergs among fast Ice

During winter and spring, icebergs, located near the outlet glacier boundaries, can be frozen into fast ice. Level fast ice is shown with uniform dark tone in SAR images, whereas deformed fast ice – with more light and not uniform tone, which changes, depending on degree of deformation [26]. Icebergs have high backscatter and are shown as bright spots among dark level fast ice. During implementation of sea ice studies in Hornsund in Svalbard in April 2004, two icebergs, 65 m and 60 m long were observed in level fast ice in several tens of meters from each other. Analysis of ENVISAT ASAR WS, and APP images (VV- and HH-polarization), shown in figure 2, revealed that in four of five analyzed ASAR WS images these icebergs were shown as bright spots. They are also evident in the APP images with 30-m resolution. However, in both cases their mapping using SAR data in absence of subsatellite observations is complicated. In spite of higher resolution in APP mode, their recognition was not more reliable, probably due to higher speckle-noise in this mode. One more 40-m long iceberg was detected only in one of five ENVISAT ASAR WS images.

A joint analysis of ENVISAT ASAR, “Monitor-E” and Landsat images allowed estimating the size of icebergs to be detected in fast ice of FJL from SAR data (Figure 3). Comparison of presented images shows, that cluster of small icebergs and growlers in the fast ice near the outlet glacier boundary (4), which is clearly seen in Landsat and “Monitor-E” images, is shown with uniform light tone in ENVISAT ASAR image, and detection of single icebergs is impossible. Seaward of these area three light points can be detected in ENVISAT ASAR image, which correspond to icebergs that are clearly detected in Landsat and “Monitor-E” images. Sizes of these icebergs estimated from 8-m resolution “Monitor-E” images amount to 185 m (1), 130 m (2), and 90 m (3).

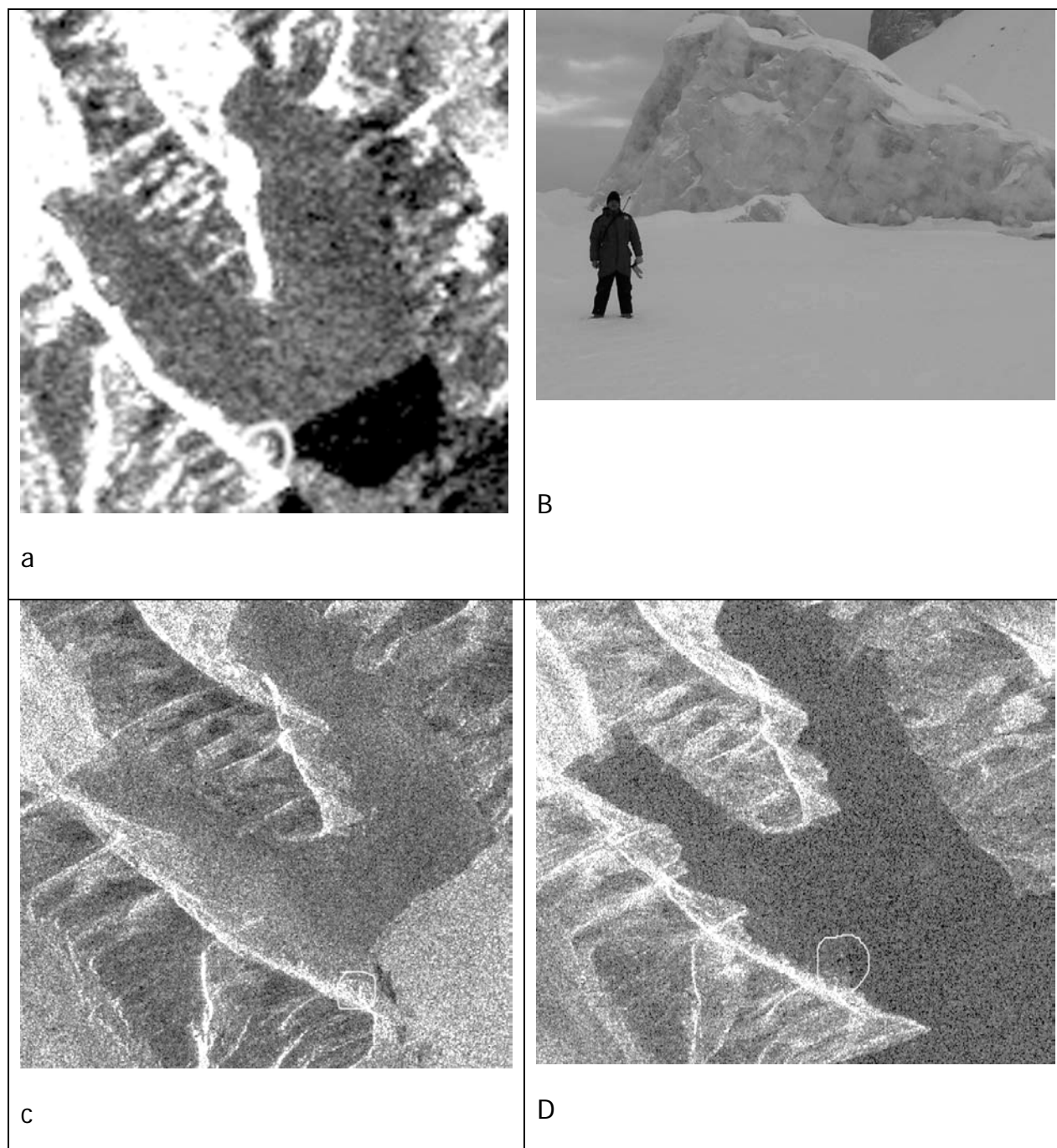
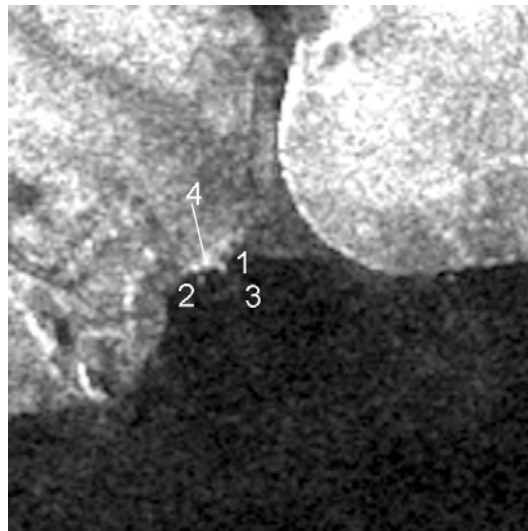
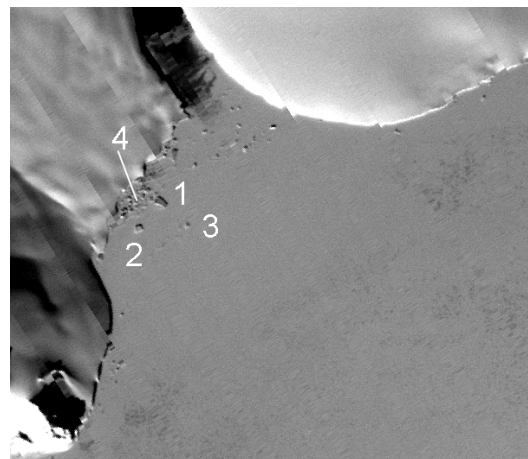


**Figure 2 ENVISAT SAR images of Hornsund area in Svalbard and photo of iceberg, April 2004. a) ASAR WS image for 01.04.2004; b) photo of observed iceberg, detected in SAR images; images in APP mode for 15.04.2004: c) – at VV-polarization and d) at HH-polarization. Bright points, corresponding to icebergs, are delineated.**

Therefore, conducted analysis shows that icebergs not less than 50 m long can be detected in level fast ice from ENVISAT ASAR WS images. However, such icebergs have radar signature similar to speckle-noise and their detection in absence of subsatellite data is complicated. Therefore, from these SAR images icebergs longer minimum 100m can be reliably detected in level fast ice.



a



b

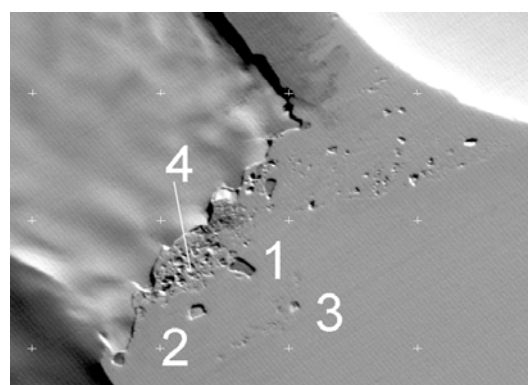


**Figure 3** Images of icebergs in fast ice of FJL. a) ENVISAT ASAR subimage for April 5, 2006, b) Landsat subimage for April 14, 2006, c) "Monitor-E" subimage for April 7, 2006.

### 3.3 Icebergs in drifting ice

The most complicated task is iceberg detection in drifting ice, because the backscatter varies significantly depending on type, form, surface state and other sea ice parameters that are characterized with significant spatial variability. In particular, characteristic peculiar feature of sea ice

SAR images is presence of relatively small areas with a high backscatter, which have signature similar to that of icebergs. Therefore, satellite visible images and subsatellite observations data should be used in analysis of iceberg detectability in SAR images.

A large number of icebergs and growlers were observed from the ships in the area of Vilkitsky strait and western Laptev Sea in September 2006. Analysis of ENVISAT IMM image for October 14, 2006 (Figure. 4a), covering an area to the west of Vilkitsky strait, allowed identification of icebergs in this area, shown as bright spots. Figure 4b shows a map of iceberg distribution, composed from this image.

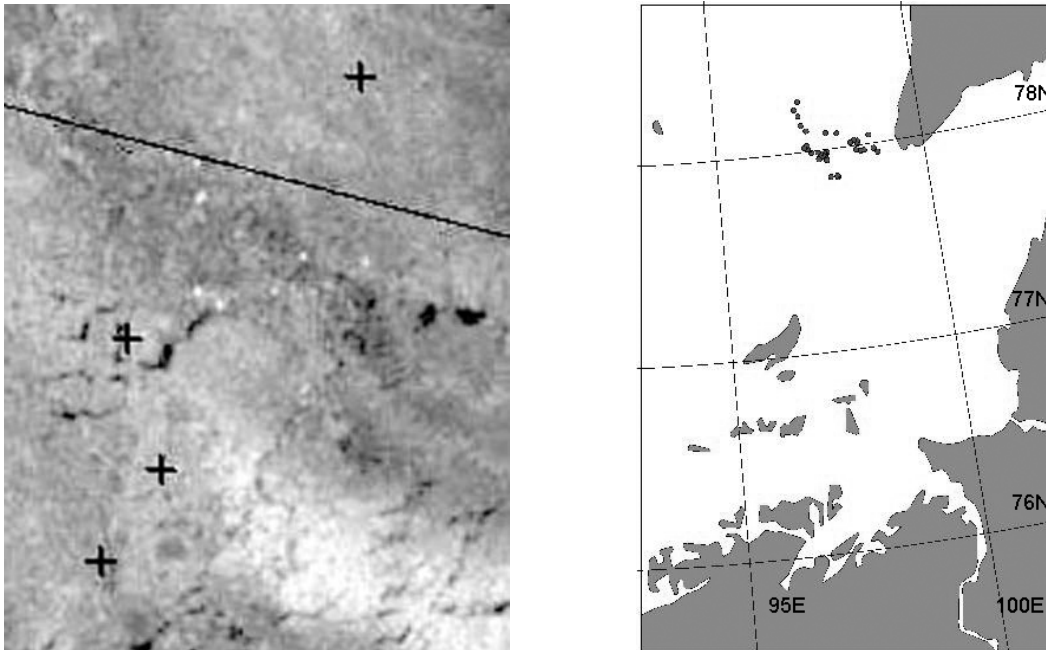


**Figure 4 ENVISAT IMM subimage, covering an area west of Vilkitsky Strait (a) and iceberg distribution map, composed from analysis of this image, October 14, 2006 (b). Crosses correspond to locations of icebergs, observed in this area in late September.**

Successive SAR images can be used to increase a probability of iceberg detection in drifting ice. Such analysis was conducted in area of Inostrantseva Bay, where a large number of icebergs and growlers was observed. They were grounded in shallow waters of this Gulf allowing comparison of their identification from images, obtained from different satellites in different time. Sea ice conditions in the area under study significantly varied in April-May 2006, that is clearly evident from SAR image analysis. The boundary between fast ice and open water is clearly evident in Landsat image. One large iceberg, which has a shadow, as well as several smaller icebergs are clearly evident in fast ice. This large iceberg can be detected also in SAR images, presented in Figure 5 (a-f). Fast ice signature in SAR images varies and location of light points, which may correspond to icebergs, varies from image to image.

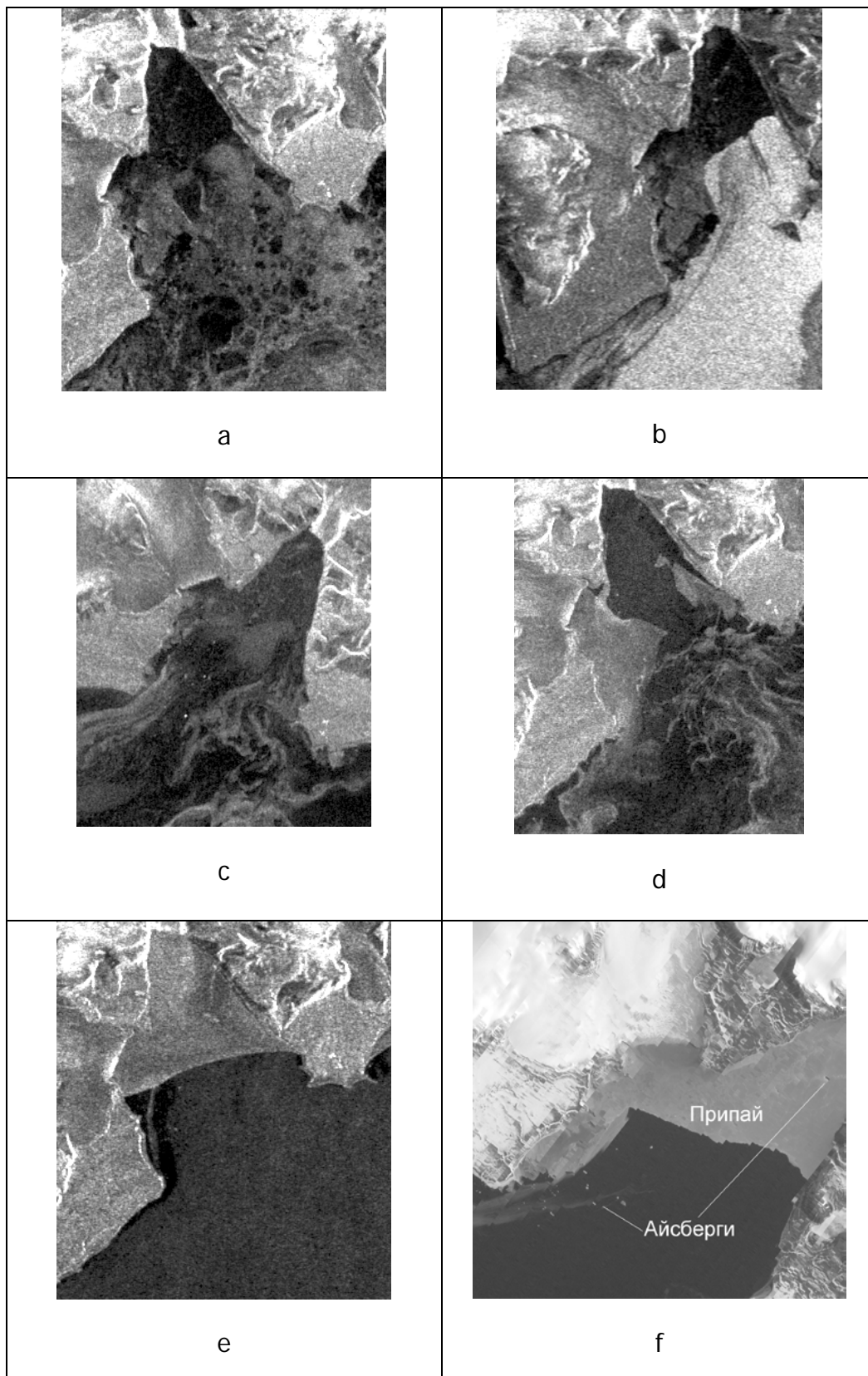


**Figure 5 Images of icebergs in Inostrantseva Bay: ENVISAT ASAR WS for March 31 (a), April 01 (b), April 18 (c), April 22 (d), April 25 (e), May 11 (f) and Landsat visible image for April 23, 2006 (g).**

Analysis of SAR image for March 31, 2006 shows that first-year ice floes and young ice located out of the fast ice boundary, and several bright points, probably, corresponding to icebergs, can be detected there. In SAR image for April 1 wind-roughened, water surface, shown with light tone, is evident in this area, which means that during this period drifting ice was advected from Inostrantsev Bay. Iceberg detection in this background is complicated. Analysis of SAR image for April 18 shows, that out of the fast ice boundary, which hardly be detected, ice formation took place and the Gulf was covered with new ice and pancake ice. Several bright points, corresponding to icebergs, are reliably detected along the northern coast of Inostrantseva Bay. Their location agrees with location of icebergs, detected in Landsat image for April 23. In SAR image for April 22 the fast ice boundary is detected reliably among wind-roughened water surface, and several icebergs can be detected along the northern coast of Inostrantseva Bay, whose location also corresponds to Landsat data. In SAR image for April 25 the fast ice boundary in the Gulf cannot be detected from wind-roughened water surface. As compared with April 23, young ice area along the northern coast of Inostrantseva Bay increased significantly and several icebergs among it can be detected as bright points. In SAR image for May 11 the fast ice in Inostrantseva Bay is shown with brighter tone compared to previous images, which is probably caused with development of ice melting, Its boundary is clearly evident from sea surface, among which several icebergs can be detected as bright points.

As a whole, this example shows that the same icebergs can be differently detected in SAR images depending on characteristics of surrounding sea ice or water surface, and analysis of successive SAR images allows obtaining more accurate data on their location.

## 4 Comparison of data on iceberg distribution, derived From satellite images with historical data

The contemporary data base of icebergs in the Arctic Seas is based on air reconnaissance data and observations from ships and polar stations. Using these data maps of iceberg distribution are composed, including maximum and average number of observed icebergs for 100 x 100 km squares and probabilities of their occurrence in different months, their interannual variability and southern boundaries of their distribution are estimated [5]. Obviously, a number of observed icebergs significantly depend on number of air reconnaissance flights and traverses that were significantly different for different years [27]. It is also obvious that data, presented in Atlas of Arctic icebergs [5] underestimate a real number of icebergs and the main question is how large are this discrepancies? The coverage of the northeastern Barents sea with three Aster images is shown in Figure 6. Totally 245 icebergs were identified in these images, each of them is 60 km x 60 km. Therefore, their average density in this area is 227 icebergs per 10,000 km<sup>2</sup>. According to the data, presented in Abramov's Atlas [5], the maximum number of icebergs, observed to the south of FJL varied from 5 to 100 per 10,000 km<sup>2</sup>, and their average number did not exceed 5. Therefore, satellite high-resolution images allows obtaining more accurate estimates of their number than historical data, based on air reconnaissance and ship observations data.

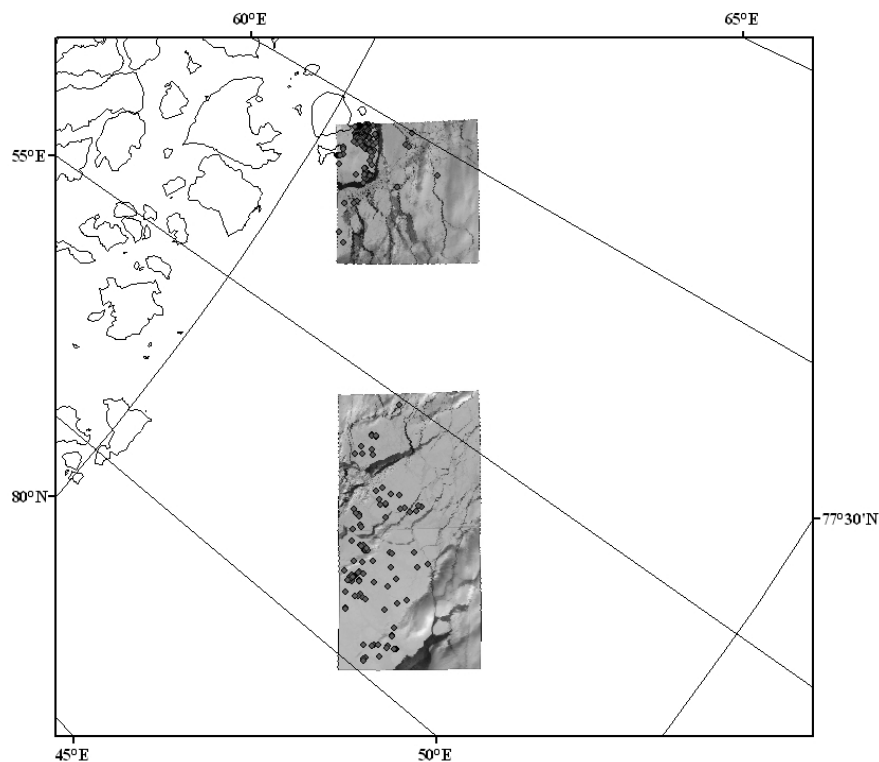


**Figure 6** Three visible Aster images for April 20, 2005, overlaid on the map of northeastern Barents Sea. Detected icebergs are marked by dots.

## 5 CONCLUSIONS

The possibility of iceberg identification in visible Landsat, "Monitor-E", Aster and MODIS images is analyzed. Preliminary estimates showed a possibility to recognize (60-90 m) long icebergs in Landsat TM images, (20-25 m) long in panchromatic and (40-50 m) long icebergs in multispectral "Monitor-E" images, (30-35 m) long icebergs in Aster images, and longer than 500 m icebergs in MODIS images. Sun height, which determines iceberg shadow, as well as contrast between sunny sight of iceberg and surroundings, influence a possibility of their identification. Conducted analysis showed that more accurate data on iceberg distribution can be derived from visible high-resolution images, than from air reconnaissance and ship observations data, used in composition of contemporary data bases.

A possibility of iceberg identification among open water, fast ice and drifting ice is analyzed. A possibility in principle of using ENVISAT ASAR data with 150 m resolution for their recognition among water surface and fast ice is shown. A minimum size of detected icebergs amounted to more than 100 m. Their recognition in drifting ice is the most complicated task. Examples of their detection in the Laptev Sea, where several hundred meters long icebergs are observed, are presented. In the Barents Sea, where size of icebergs is less, their detection in SAR images is more ambiguous.

Development of iceberg detection methodology depends not only on improvement of technical means of their observations from space, namely improvement of resolution, and operativeness of their reception. At present time, combined use of different types of satellite information depending on ice and hydrometeorological conditions in the area under study, and successive image analysis allows significant improvement of iceberg identification reliability.

## 6 References

1. *Govorukha L.S.* Contemporary land glaciation of the Soviet Arctic. Leningrad, Gidrometeoizdat, 1989, 256 p. (in Russian).
2. *Kloster K. and Spring W.* Iceberg mapping using satellite optical imagery during the Barents sea ice acquisition program (IDAP). Proceedings of the Twelfth Conference on Port and Ocean Engineering under Arctic Conditions (POAC'93), Hamburg, Germany, 17-20 August 1993 (Hamburg: Hamburg Ship Building Basin (HSVA), Department for Ice and Environmental Monitoring), 1993, p. 413-424.
3. *Loiset S.* Drift and volume estimation of icebergs in the Barents Sea. Proceedings of Naturdatakonferanse Harstad 26-28 September 1989, p. 220-236.
4. *Sharov A.I.* Satellite Hydrographic Monitoring and Assessment of Environmental Trends along the Russian Arctic Coast (AMETHYST). Final Scientific Report, Joanneum Research, 2002, 148 p.
5. *Abramov V.* Atlas of Arctic Icebergs, The Greenland, Barents, Kara, Laptev, East-Siberian and Chukchi Seas and the Arctic Basin. NJ, USA, Backbone Publishing Company, 1996, 70 p.
6. *Vinje T.* Physical environment western Barents Sea. Drift, composition, morphology and distribution of the sea ice fields in the Barents Sea. Skrifter Nr. 179C, Norskpolarinstitutt, Oslo, 1985, 26 p.
7. *Vefsnmo S., Lovas S.M., Loiset S., and Nass T.* Identification and volume estimation of icebergs by remote sensing in the Barents Sea. Proceedings of the International Geoscience and Remote Sensing Symposium '89 – Twelfth Canadian Symposium on Remote Sensing: An Economic Tool for the Nineties, Vancouver, Canada, 10-14 July 1989, Ottawa, 1989, p. 2355-2358.
8. *Volkov V. and Vinje T.* Cruise report R/V Akademik Shuleykin 24.07-14.08.1989. Norsk Polarinstitutt, Rapportserie, Nr. 57, Oslo, 1990, 16 p.
9. *Johnsen A.S and, Vinje T.* IDAP-89. Russian buoy deployment. Volume 1: Field observations and first period analysis. Norsk Polarinstitutt, Oslo, 1990, 37 p.
10. *Pavlov V., Foldvik A., Ivanov B., and Vinje T.* Soviet-Norwegian Oceanographic Programme 1988-1992. Cruise Reports 1990. Rapportserie Nr.73, Norsk Polarinstitutt, Oslo, 1991, 87 p.
11. *Vinje T. and Volkov V.* Cruise Reports 1991. Rapportserie Nr.78, Norsk Polarinstitutt, Oslo 1992, 80 pp.
12. *Zubakin G.K., Naumov A.K., and Buzin I.V.* Estimates of ice and iceberg spreading in the Barents Sea, Paper No. 2004-JSC-381, 2004, p.1-8.
13. *Naumov A.K.* Iceberg distribution in the area of Shtokman gas-condense deposit and estimates of probability of their collision with a platform. AARI Transactions, vol, 449, 2004, p. 140-152.
14. *Demytyev A.A.* Climatic conditions of iceberg formation and drift in the Barents and Kara Seas. AARI Transactions, vol. 439, 1998, p. 197-215.
15. *Bushuev A.V., Bychenkov Yu.D., Loshchilov V.S., and Masanov A.D.* Ice cover study by means of side-looking airborne radar (SLAR) stations. Methodological manual, 120 pp. Gidrometeoizdat, Leningrad, 1983 [in Russian].
16. *Alexandrov V.Y., Johannessen O.M., and Sandven S.* SAR sea ice monitoring in the Arctic. In: A. Pasmurov and J. Zinoviev "Radar Imaging and Holography". Chapter 9.1.2. . Stevenage, Herts, UK, The Institution of Electrical Engineers, Michael Faraday House2005, p. 191-204.

17. *Partington, K.C., Boakes, K.P., Oddy, C.J., Sephton, A.J., Walker, N.P. and Willis, C.J.* An image analysis system for the production of sea ice maps from space. *GEC Journal of Research*, Vol. 11, No. 3, 1994, p. 141-149.
18. *Willis, C.J., Macklin, J.T., Partington, K.C., Teleki, K.A., Rees, W.G. and Williams, R.G.* Iceberg detection using ERS-1 Synthetic Aperture Radar. *International Journal of Remote Sensing* vol. 17, No. 9, 1996, p.1777-1795.
19. *Power D., Youden J., Lane K., Randell C, and Flett D.* Iceberg detection capabilities of RADARSAT Synthetic Aperture Radar. *Canadian Journal of Remote Sensing*, vol. 27, No. 5, 2001, p. 476-486.
20. *Johannessen O.M., Sandven S., Drottning A., Kloster K., Hamre T., and Miles M.* ERS-1 SAR Sea Ice Catalogue. Noordwijk, the Netherlands, ESA Publications Division, ESTEC, 1997, 89 p.
21. *Sandven S., Johannessen O.M., Miles M.W., Pettersson L.H., and Kloster K.* Barents sea seasonal ice zone features and processes from ERS-1 synthetic aperture radar: Seasonal Ice Zone Experiment 1992. *Journal of Geophysical Research* vol. 104, No. C7, 1999, p. 15843-15857.
22. *Alexandrov, V.Y., Loshchilov, V.S., and Provorkin, A.V.* (1996) Studies of icebergs and sea ice in Antarctic using *Almaz-1* SAR data, In: Popov, I.K. and Voevodin, V.A. (eds), *Icebergs of the World Ocean*, pp. 30-36. Gidrometeoizdat, St.Petersburg, [in Russian].
23. *Onstott R.G.* Antarctic Sea Ice and Icebergs. Chapter 19 in C.R. Jackson and J.R. Apel (eds) *Synthetic Aperture Radar Marine User's Manual*. US Department of Commerce, NOAA, 2004, p. 397-415.
24. *Sephton A.J. and Partington K.C.* Towards operational monitoring of Arctic Sea Ice by SAR. In: Tsatsoulis, C. and Kwok, R. (eds), *Analysis of SAR Data of the Polar Oceans*. Recent Advances. Berlin. Springer-Verlag, 1998, p. 259-279.
25. *Sandven S. and Johannessen O.M.* The use of microwave remote sensing for sea ice studies in the Barents Sea. *ISPRS Journal of Photogrammetry and Remote Sensing*, vol. 48, no. 1, 1993, p.2-18.
26. *Johannessen O.M., Alexandrov V.Y., Frolov I.Y., Sandven S., Pettersson L.H., Bobylev L.P., Kloster K., Smirnov V.G., Mironov Y.U., and Babich N.G.* Remote Sensing of Sea Ice in the Northern Sea Route: Studies and Applications. Chichester, UK, Springer-Praxis, 2007, 472 p.
27. *Abramov V. and Zubakin G.K.* Russian iceberg observations 1970-1989. OKN report, 1992.

**END OF DOCUMENT**